Design and Fabrication of Liquid Pressure Sensor Using FBG Sensor Through Seesaw Hinge Mechanism

Venkata Satya Chidambara Swamy Vaddadi, *Student Member, IEEE*, Saidi Reddy Parne, *Member, IEEE*, Vijeesh V. P., Suman Gandi, Saran Srihari Sripada Panda, and Linga Reddy Cenkeramaddi, *Senior Member, IEEE*

***Abstract*—Pressure sensors are used in various industrial applications assisting in preventing unintended disasters. This paper presents the design and fabrication of a novel Seesaw device incorporating a diaphragm and Fiber Bragg Grating (FBG) sensor to measure the pressure of liquids. The designed sensor has been tested in a static water column. The proposed design enables the user to easily make and modify the diaphragm based on the required pressure range without interfering with the FBG sensor. The developed pressure sensor produces improved accuracy and sensitivity to applied liquid pressure in both low and high-pressure ranges without requiring sophisticated sensor construction. A finite element analysis has been performed on the diaphragm and on the entire structure at 10 bar pressure. The deformation of the diaphragm is comparable to theoretical deformation levels. A copper diaphragm with a thickness of 0.25 mm is used in the experiments. All experiments are performed in the elastic region of the diaphragm. The sensor's sensitivity as 19.244 nm/MPa with the linearity of 99.64% is obtained based on the experiments. Also, the proposed sensor's performance is compared with recently reported pressure sensors.**

***Index Terms*—3-D printing, Acrylonitrile-Butadlene-Styrene (ABS), diaphragm, Fiber Bragg Grating (FBG) sensor, seesaw mechanism.**

I. Introduction

PRESSURE sensors are essential in a variety of applications, including high-pressure measurements in maritime applications, the oil industry, and gas pipeline monitoring. Furthermore, aeronautical, medicinal, and wind turbine applications are the most critical applications required to correctly monitor pressure. High temperature, electromagnetic interference, and corrosion are the main drawbacks in conventional sensors such as electrical strain gauges. While the physical and mechanical properties of Fiber Bragg Grating (FBG) sensors are most appealing because they are small in size, chemically inert, good response rate, free from electromagnetic interference (EMI), dielectric, non-flammable, and non-corrosive. Due to these unique properties, they can be used in any of the above mentioned critical applications [1], [2], [3], [4]. We can achieve this through the merits and unique qualities of FBG, which can be utilized to measure various physical parameters such as temperature, pressure, liquid density, strain, and liquid level, among others [5], [6], [7]. As a result, the design and manufacture of novel types of pressure sensors is gaining attraction in the research community. Most FBG-based pressure sensors arises temperature-dependent but very sensitive to strain changes caused by applied pressure [8], [9]. Multiple FBG sensors can be written in a single optical fiber for remote sensing applications such as quasi distributed pressure monitoring in the oil and natural gas fields, thanks to the advantages of optical fiber sensing technology [10]. We can measure pressure using bare FBG sensors, but their sensitivity falls well short of the actual needs [11]. These are also fragile, willowy, and wide-open as a result of these characteristics. Pressure sensitivity with bare FBG sensors is low, hence packaging techniques must be used to improve sensitivity. To improve the sensitivity and sensitizing of pressure using FBG sensors, different types of packaging technologies have been implemented, such as embedding the FBG in 3-D printed Poly Lactic Acid (PLA) material [12], using elastic materials such as metal cantilever beams [13], metal diaphragms [14], [15], [16], bourdon tubes [17], are developed to produce pressure sensors in actual measurements. These methods improved the sensitivity of the sensor, but FBG sensors are sensitive to temperature also. Therefore, there is cross talk between temperature and pressure during measurements, leading to false pressure values. Accordingly, to compensate temperature while measuring pressure, temperature compensation solutions have been developed by the researchers, such as using two FBG sensors [18], using different coatings on FBG sensors [19], Fabry-Perot (FP) cavity sensors [20]. Cui et al. developed a dual cavity Fabry - Perot interferometer for the simultaneous measurement of temperature and pressure measurement [21]. In this work, they achieved good results in a large measurement range, but these interferometry-based sensors are difficult to multiplex and require stable laser sources

Manuscript received 11 June 2022; revised 3 September 2022; accepted 24 September 2022. Date of publication 27 September 2022; date of current version 4 October 2022. This work was supported by Indo-Norwegian collaboration in Autonomous Cyber-Physical Systems under Project 287918 of International Partnerships for Excellent Education, Research and Innovation Program from the Research Council of Norway. *(Corresponding author: Linga Reddy Cenkeramaddi.)*

Venkata Satya Chidambara Swamy Vaddadi, Saidi Reddy Parne, Vijeesh V. P., Suman Gandi, and Saran Srihari Sripada Panda are with the Department of Applied Science, National Institute of Technology Goa, Ponda 403401, India (e-mail: swamych@nitgoa.ac.in; psreddy@nitgoa.ac.in; vijeesh@nitgoa.ac.in; gandisuman@nitgoa.ac.in; saranpanda6@gmail.com).

Linga Reddy Cenkeramaddi is with the Autonomous and Cyber-Physical Systems (ACPS) Research Group, Department of Information and Communication Technology, University of Agder, 4879 Grimstad, Norway (e-mail: linga.cenkeramaddi@uia.no).

Digital Object Identifier 10.1109/JPHOT.2022.3210146

for data acquisition system. By using 3-D printing technology, Luca Schenato et al. developed a prototype FBG based pressure sensor for underground water level monitoring [22]. Fan et al. reported a square diaphragm type FBG based sensor for pressure measurement, here they achieved low sensitivity with good linearity 99.996% [23]. To improve the sensor's sensitivity, Vengal Rao et al. have done a chemical etching process on the fiber clad part. With this process, they reported good sensitivity, which is 18870 times more than bare FBG sensitivity [24]. A group of researchers developed the new type of pressure sensor by using PLA (Poly Lactic Acid) material, and 3-D printing technology [25]. In this design, they have embedded the sensor inside the 3-D fabricated material. By this method, the reported sensor sensitivity is 13.22 kPa/pm.

In this article, a novel pressure sensor using 3-D printing technology by using ABS as a printing material is designed and pre fabricated. Proposed sensor design produce high sensitivity and good repeatability. In this design, diaphragm and the Seesaw mechanism plays a vital role because outside pressure directly acts on the diaphragm. Instead of a battery-powered sensor, the Seesaw mechanism used to be employed to monitor tire pressure for the automotive industry. To the best of our knowledge, a Seesaw mechanism-based optical pressure sensor for applications requiring underwater column pressure detection has been created for the first time. This novel Seesaw approach enhances the sensor's sensitivity, linearity, and reliability. However, there is a trade-off between measurement range and sensor sensitivity. Here, 3-D printing technology has been selected to create the sensor at a lower cost, for quick testing and prototyping. A simulation studies have been done on copper material diaphragm with thickness of 0.25 mm under 10 bar pressure. Also, the full-body simulation has been done to understand the designed structure. The designed sensor has been tested three times in 5 meters static water column, which is having a constant temperature.

The remainder of this article has been arranged as follows. Section II describes about FBG sensor, working principle, proposed design and implementation of Seesaw mechanism with mathematics and structural analysis of the sensor. Section III describes about the simulation studies on the metal diaphragm and on total structure. Section IV shows the experimental results of the sensor in a 5 m static water column. Finally, Section V discuss about the conclusions and future work.

II. Sensor Fabrication

A. Working Principle of FBG Sensor

The FBG sensor is an optical-based sensing device that was created to quantify temperature, strain, and pressure with regard to wavelength shift. FBG is frequently used in telecommunication and in different sensor technologies. Gratings are formed by periodic change in the core of the fiber in the direction of propagation of optical radiation. FBG works based on the principle of Bragg reflection, Fig. 1 shows the schematic diagram of basic working principle of FBG. It works as a spectral filter, i. e., when a broadband light passes through FBG, it reflects a particular wavelength which satisfies the Bragg's condition and remaining light transmits through it. The Bragg's condition for

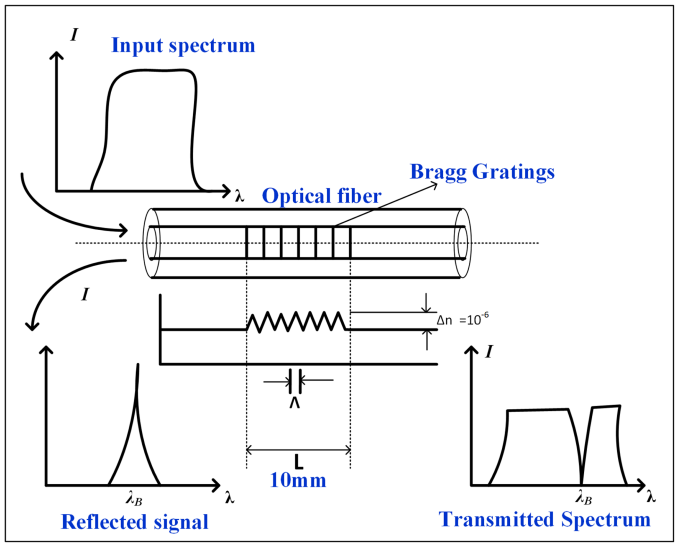

Fig. 1. Operation principle of FBG sensor.

the reflected light signal is defined as follows [26]:

$$\lambda_B = 2n_{eff}\Lambda \tag{1}$$

Where 'λ_B' is central Bragg wavelength, 'n_{eff}' is the effective refractive index of the fiber core mode supported by the optical fiber at the central Bragg wavelength, and 'Λ' is periodicity of grating. If an external interruptions is applied on FBG, such as temperature, pressure, and strain, then there is a shift in central wavelength. The effective refractive index of the core and grating period are the main factors. These two parameters gets modulated if there is an interference from external sources, which computes a shift in the central wavelength of the FBG. The shift in the central wavelength caused by temperature and strain is expound as [1]:

$$\frac{\Delta\lambda_B}{\lambda_B} = (1 - p_e)\epsilon + (\alpha + \zeta)\Delta T \tag{2}$$

where 'p_e' is the effective photo-elastic coefficient of the fiber, which is equal to 0.22, 'α' is thermal expansion coefficient, 'ζ' is a thermo-optic coefficient, 'ϵ' is axial strain in the fiber, and 'ΔT' is variation in acting temperature on fiber. From the above equation, it is understand that the shift in the central wavelength is dependent on both temperature and strain. In this design, FBG sensor is packed inside the sensor head such way that end parts of the sensor only glued with cyanoacrylate adhesive. Following that, the body of the sensor head is sealed without any leaks, and no contact of measuring physical parameters of the water (i.e., temperature, density, salinity) with the FBG sensor occurs. As a result, our system only detects the water pressure acting on the diaphragm surface. The designed sensor head is tested in a static water column with a constant water body temperature. Thus, the second term is neglected, which arises from temperature change. Then (2) is converted into:

$$\frac{\Delta\lambda_B}{\lambda_B} = (1 - p_e)\epsilon \tag{3}$$

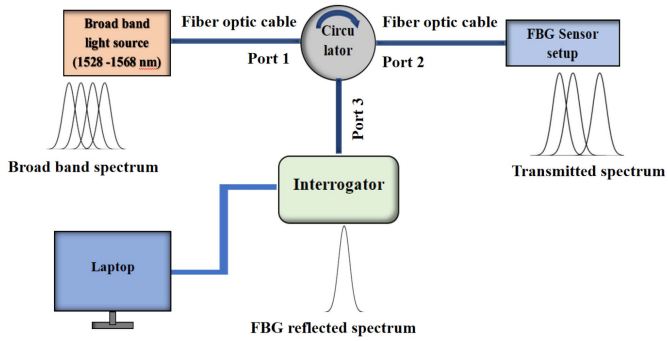

Fig. 2. FBG sensor interrogation mechanism.

TABLE I
FBG SENSOR PARAMETERS

S. No.	Parameters	Details
1	Used fiber	SMF-28
2	Writing method	Phase mask
3	Central wavelength	1554 nm
4	Period of the grating	508.86 nm
5	Coating type	Acrylic
6	FWHM (Full width at half maximum)	0.3 nm
7	Reflectivity	80%(Approx.)
8	Length of the FBG	1 cm

B. FBG Sensor and Interrogation Mechanism

Fig. 2 shows the block diagram of the FBG sensor interrogation mechanism. A commercially available Smartscan interrogator is used in this experiment. It was equipped with a C -band tunable laser source with a bandwidth of 40 nm in the range of 1528-1568 nm, which can measure the wavelength shift with 1 pm bandwidth resolution. In this interrogator, a 3 - port optical circulator is used, which can restrict the back reflections in the circuit. When a broadband light is launched from the source, it travels through circulator port 1 and enters the FBG sensor network through port 2. The reflected light from the FBG sensor network is redirected to circulator port 3, where it is routed to the processing unit. The data processing unit (DPU) will capture the reflected light signal using Smartsoft interrogation software, which operates using the LabView user interface. The T10 model FBG used in this experiment was obtained from Technicasa, and complete sensor details are tabulated in Table I.

C. Proposed Novel Seesaw Mechanism

Fig. 3 shows the schematic diagram, and Fig. 4 shows the free-body diagram of the Seesaw mechanism. From the Fig. 3, T is tension developed in the FBG sensor, and F is the force due to liquid or air pressure. In the actual Seesaw mechanism, arm length is the same. In case of proposed design, to increase the sensor sensitivity, the mechanical Seesaw lever is fixed so that the length of the arms is uneven. Such that the FBG is fixed at the shorter length side and pressure applied at the longer length side. From the free body diagram, a =2b. Taking a moment of

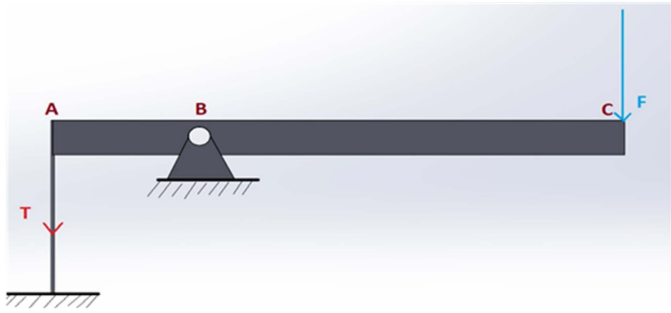

Fig. 3. Seesaw mechanism.

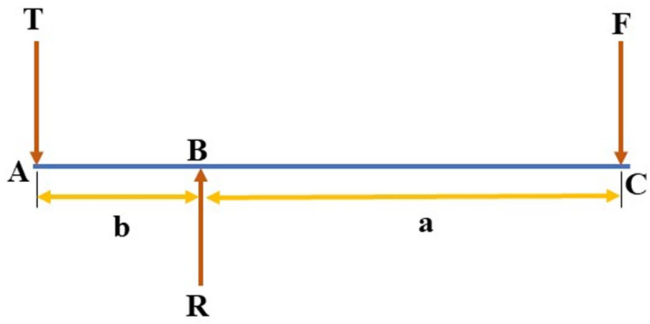

Fig. 4. Free body diagram of the Seesaw mechanism.

inertia into account at B

$$\Sigma M_B = Fa - Tb = 0$$
$$\Rightarrow 2F = T(\because a = 2b) \quad (4)$$

From the above analogy tension in the fiber is doubled by applied force. This gives more sensitivity to the sensor even at small pressure range as well as at high pressure application.

D. Mechanical Analysis of the Sensor Structure

To meet the measurement requirements, the sensor must fulfill the following 1. Easy to fabricate, 2. Durability, 3. Long term service stability, 4. Low maintenance cost, is needed for the pressure measurement. The sensor module majorly includes of a metal diaphragm, FBG, and the Seesaw mechanism. Here FBG is glued in between one side of the Seesaw lever face and 3-D printed body. The other side of the lever, a rod is connected to it from the bottom of the diaphragm. Here the seesaw mechanism is a key component since it will double the strain in the FBG with applied pressure. From small deformation theory, when liquid pressure or air pressure applied on the circular flat diaphragm, maximum deflection crop up at the midpoint of the diaphragm and minimum at its edges. The diaphragm deformations and real time alterations are done by using ANSYS FEM simulation software. Diaphragm deformations are calculated theoretically by [27]:

$$D = \frac{qr^4}{64\,K} \quad (5)$$

where 'D' is deformation of the used diaphragm due to applied pressure, 'q' is applied pressure on the diaphragm, 'r' is radius of the diaphragm and 'K' is bending stiffness of the diaphragm which is given by [27]:

$$K = \frac{Eh^3}{12(1-\mu^2)} \tag{6}$$

where 'E' is the young's modulus, 'μ' is Poisson's ratio, and 'h' is the thickness of the diaphragm. Strain in the FBG is calculated by taking two assumptions. The first one is, when load applied on the diaphragm it directly transfers to the rod without any degradation. The second assumption is, there is no bending moment of FBG. The translation moment of the FBG is considered here with applied pressure. Therefore, wavelength shift with respect to applied pressure is

$$\Delta\lambda_B = \lambda_B[(1-p_e)\epsilon_f] \tag{7}$$

$$\epsilon_f = \frac{F_f}{A_f E_f} \tag{8}$$

where 'ϵ_f' is strain in the FBG sensor, 'F_f' is force on FBG sensor, 'A_f' is cross sectional area, and 'E_f' is young's modulus of the used optical fiber.

$$F_f = \frac{\Delta\lambda_B A_f E_f}{\lambda_B(1-p_e)} \tag{9}$$

From the below Seesaw mechanism, force applied on the diaphragm is half of the force at FBG sensor. Since the ratio of arm length is fixed as 2:1. Therefore,

$$F_d = \frac{F_f}{2} \tag{10}$$

$$F_d = P.a \tag{11}$$

where 'P' is applied pressure on the diaphragm, and 'a' is area of the diaphragm

$$P = \frac{F_f}{2a} \tag{12}$$

$$P = \frac{\Delta\lambda_B A_f E_f}{\lambda_B(1-p_e)2a} \tag{13}$$

III. Sensor Head Design and Modelling

Diaphragm based pressure transducers with FBG sensors have been designed, tested and reported [28], [29]. The Young's modulus of the copper diaphragm material is much greater than the silica fiber, and same for the gratings. Therefore, the physical properties of the diaphragm play a vital role in the calculation of wavelength shift from the gratings. Therefore, ANSYS Finite element analysis (FEA) has been carried out on the diaphragm material to evaluate the proposed sensor design's performance and to compute the FBG sensor sensitivity. A copper diaphragm with a thickness of 0.25 mm, a diameter of 30 mm is chosen as a pressure transducer. To study the diaphragm deformations, a 10 bar pressure is applied on surface of the diaphragm. As applied pressure increases on the surface of the diaphragm, the maximum deformation occur at it's center and which can be clearly seen in Fig. 5. These simulation studies can briefly describe the suitable diaphragm for the required pressure range. The diaphragm simulations are divided into two stages. In the first stage, a solid model is created and did the global analysis on it, in the second stage, done the diaphragm deformation analysis in detail with the help of the first one.

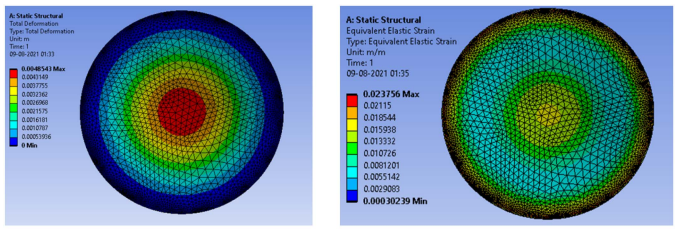

(a) (b)

Fig. 5. Simulation results of copper diaphragm with thickness of 0.25 mm under 10 bar pressure (a) Deflection profile, (b) Strain profile.

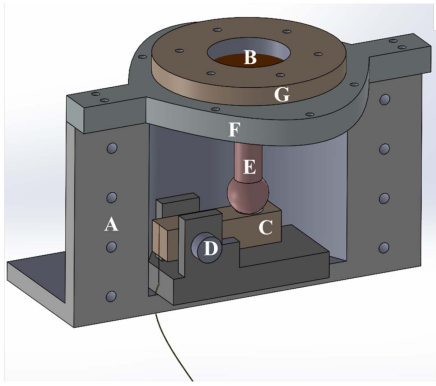

Fig. 6. Front view of solid model of the designed sensor head.

Results of diaphragm simulation studies are shown in Fig. 5(a) and (b). The maximum deformation of the copper diaphragm is 4.85 mm under 10 bar applied pressure, which is shown in Fig. 5(a). The maximum strain induced at the clamped edges of the diaphragm and it is shown in Fig. 5(b). Fig. 6 shows a front view of solid model of the designed sensor head. In this figure, each part is represented with an alphabetical letters from A - G. 'A' represents the outer body of the sensor head, 'B' is the metal (Copper) diaphragm, 'C' is the Seesaw mechanism rod, 'D' is a circular pin, 'E' is a cylindrical rod, 'F' and 'G' are the top covers of the sensor. The simulation analysis has been done on the sensor design after fixing all components with applied pressure. In this simulation analysis, desired constraints are given on parts to get accurate simulation results, and considered only copper plate to show the bending moment. From Fig. 7 it is seen that maximum strain is applied on FBG when pressure acts on the metal diaphragm of the sensor head. Diaphragm properties such as deformation under pressure are mentioned in Table II.

IV. Experimentation and Results

Fig. 8 shows assembled front view of the 3-D printed sensor head. The experimental sensor head and all parts of the proposed sensor design is made with a 3-D printer using ABS (Thermoplastic) material. The 3-D printing parameters of the sensor

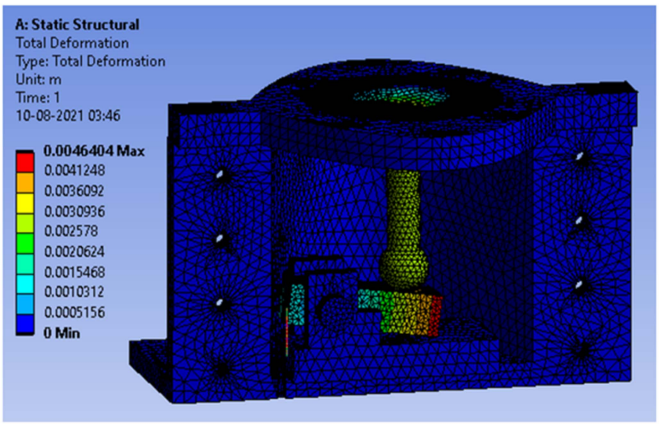

Fig. 7. Simulation of designed pressure sensor head with applied pressure.

TABLE II
DIAPHRAGM PROPERTIES

S. No.	Parameters	Material
1	Diaphragm material	Copper
2	Diameter	30mm
3	Thickness	0.25 mm
4	Applied pressure	10 bar
5	Deflection (Theory)	4.207 mm
6	Deflection (ANSYS)	4.85 mm
7	Young's modulus	128 GPa

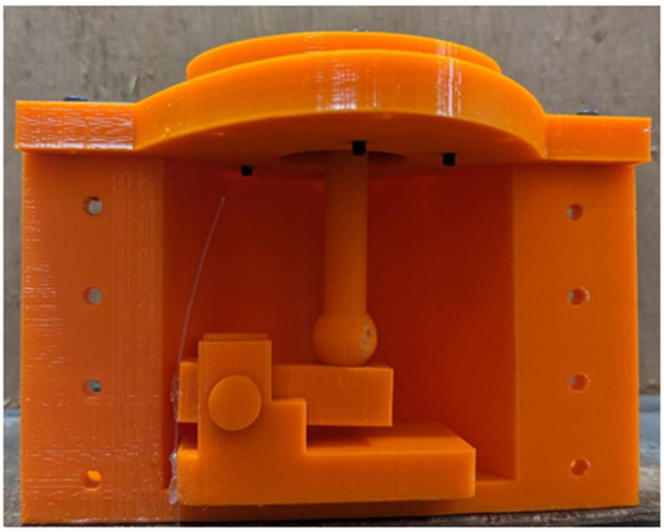

Fig. 8. Assembled open view of the 3-D printed sensor head.

head are shown in the Table III. 3-D printing or additive manufacturing technology creates three dimensional objects instead of subtraction process. This process has number of advantages including better precision, no waste of the material, reduced tool wear, and no need to cut the parts. Also, this process gives the rapid prototyping of any unconventional designs. The proposed sensor design can give more sensitivity than the existing sensors since this is working on the principle of the Seesaw hinge mechanism. Here in this design, one can easily replace or modify any sensor part according to pressure range, and assembling the sensor is simple. Different parts of the sensor head are explained

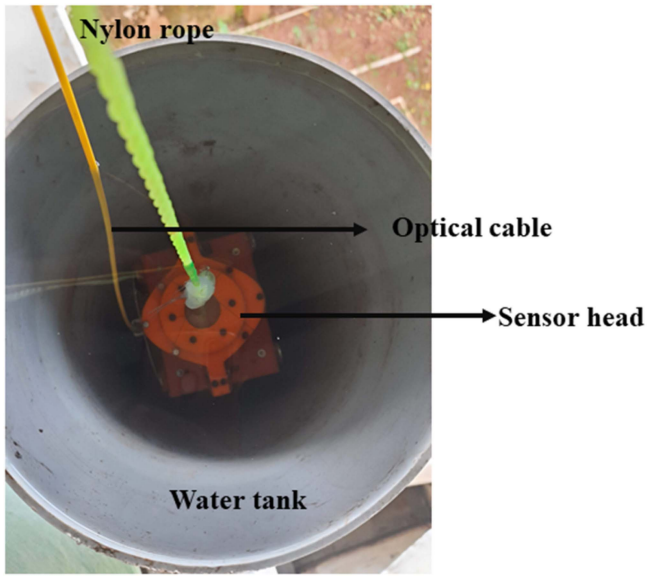

Fig. 9. Experimental setup to measure the pressure.

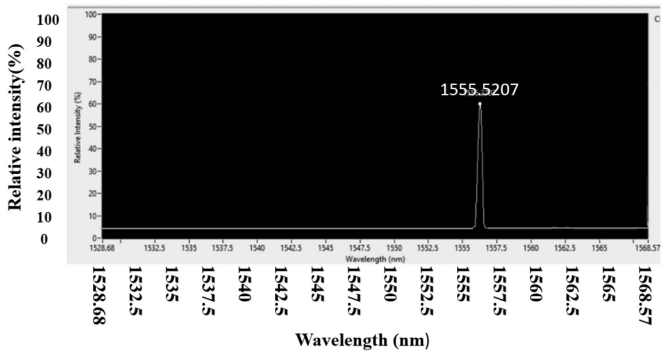

Fig. 10. Reflected spectrum of the FBG sensor.

TABLE III
PRINTING PARAMETERS

S. No.		
1	Used Material	ABS
2	Printing Density	90%
3	Bed temperature	90^oC
4	Filament temperature	180^oC

in the previous section with notations. The Seesaw mechanism plays a vital role in getting high sensitivity and repeatability in this design. Components used in this mechanism are considered as friction-less.

When the liquid pressure acts on the metal diaphragm (B), it gets deformed, and there is a rod (E) glued to the diaphragm on the bottom side. Due to deformation in the diaphragm, the rod moves downward. The tip of the rod is made as a spherical shape to make point contact with one end of the Seesaw lever. Another end part of this lever is hinged with a non-movable and rotational pivot pin. Therefore lever will move up and down according to the pressure acting on the diaphragm, which we defined as a Seesaw mechanism. One end of the FBG sensor is fixed on the Seesaw mechanism rod, and another end of the FBG is glued on the fixed part of the sensor body with cyanoacrylate glue. When

TABLE IV
COMPARISON OF VARIOUS PRESSURE SENSORS

S. No.	Authors	Design or Method	Sensitivity	Linearity	Reference
1.	C A F Marques et al.	Silicon rubber diaphragm	96×10^{3} nm/MPa	NA	[31]
2.	Min-fu Liang et al.	Diaphragm with cantilever	0.339 nm/MPa	99.997%	[13]
3.	Jun Huang et al.	Diaphragm type	0.00321 nm/MPa	99.98 %	[32]
4.	Marcel Fazkus et al.	3D printed Diaphragm	0.9086 nm/MPa	99.82 %	[33]
5.	Gray Allwood et al.	Circular Rubber membrane	0.116 nm/MPa	NA	[34]
6.	E. Vorathin et al.	Natural Rubber membrane	0.1007 nm/kPa	99.73 %	[35]
7.	Yanling Xiong et al.	Flat diaphragm	2.3×10^{-3} nm/MPa	97.20 %	[29]
8.	This work	Metal Diaphragm	19.2440 nm/MPa	99.64 %	

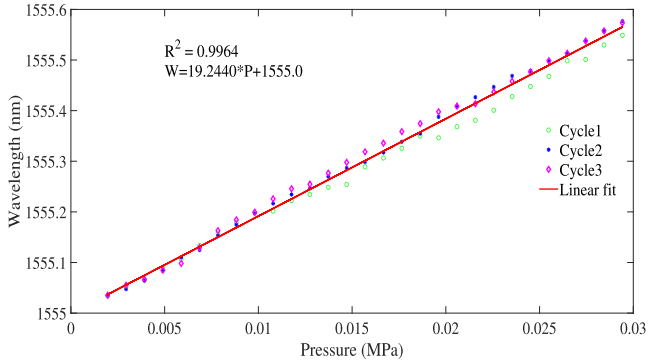

Fig. 11. Graph between applied pressure and wavelength shift.

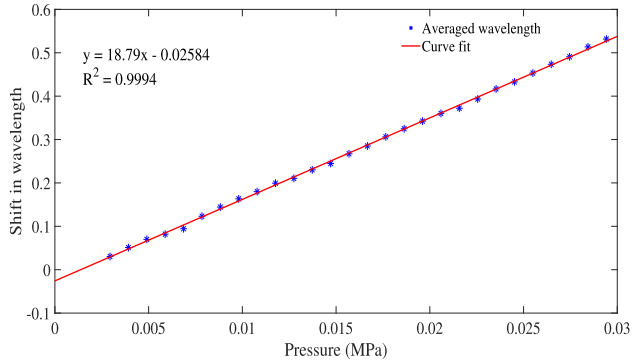

Fig. 12. Graph between applied pressure and shift in averaged wavelength.

the pressure is applied on the diaphragm, the rod which is glued on the bottom side of the diaphragm moves downward, and it acts as a force on the Seesaw mechanism rod, which turns the strain in FBG corresponding to the pressure variation. Pressure on the diaphragm increases as the depth of water increases. Due to strain in the FBG sensor, a shift in wavelength occurs. The shift in wavelength from the FBG sensor is measured by using reflected spectra through an optical interrogator. The reflected spectra from the FBG sensor is shown in Fig. 10. For each 10 cm water depth, the wavelength shift is measured and is converted in terms of pressure using (13). The applied pressure for every 1-meter depth is 0.01 MPa [30]. The whole mechanism is covered with another 3-D printed half hollow circle part, and both of these parts are joined with hot glue so that FBG sensor is not in contact with water. The designed sensor head is tested in a 5-meter water column, and the experimental setup is shown in Fig. 9.

From Table IV the different types of pressure sensors are compared with present designed sensor. Researchers have developed various pressure sensors with several diaphragm materials. Some of these designs achieved good sensitivity when compared with our design. But these diaphragm materials can not withstand at high-pressure range. In present design, the diaphragm will measure the pressure up to 3-meters depth of the water with good linearity and repeatability. Other methods with diaphragms reported less sensitivity than our proposed sensor design. Experimentation done by dipping the 3-D printed sensor head in a water tank up to 3-meters depth by hand with the help of a plastic rope which has scale marks for each 10 cm length, and wavelength shift is measured for every 10 cm depth of water. The experimentation is performed three times by dipping and taking out the sensor head. The data has been collected while dipping and taking out time. The average of the data for each

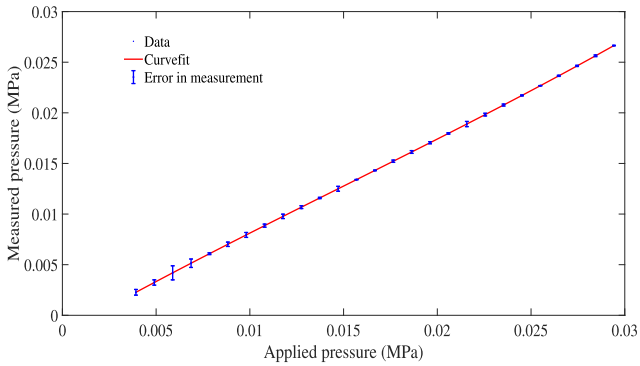

Fig. 13. Graph between applied pressure and measured pressure.

cycle and plotted in Fig. 11. Pressure is measured for three times in the tank, and wavelength shift is noted for all three cycles. The graph shows good repeatability of the designed sensor, and calculated sensor sensitivity is 19.24 nm/MPa with a correlation coefficient 0.9964. From the above data average wavelengths for each depth of 10 cm from all three cycles is measured and it is plotted against the pressure, which is shown in Fig. 12. From this graph it is clearly noted that the total wavelength shift is 0.6 nm for the applied pressure, and fit from this graph increased the sensors correlation coefficient. Fig. 13 shows the error graph between applied pressure and measured pressure for each 10 cm of water depth. From this graph, it is noted that the designed sensor is capable to measure the pressure with less errors.

V. CONCLUSION

In this work, a liquid pressure sensor using FBG sensor has been designed and fabricated. The designed pressure sensor

can measure up to 0.03 MPa with 0.25 mm thickness of the copper diaphragm. By changing the diaphragm thickness, it is possible to measure lower and higher pressure ranges with good accuracy. Theoretical deformation of the proposed diaphragm values is in line with simulation deformation. Based on the experiments, the proposed sensor with printing density of 99% can measure pressure with good accuracy and sensitivity and for high pressure range experiments one need to change the outer material of the sensor head. The experiment results indicate that the proposed FBG sensor produces high-pressure sensitivity of 19.244 nm/MPa with good repeatability and good linearity with a linear fitting coefficient of 99.64%. The main advantage of this sensor is that 3-D printing technology was used for sensor fabrication to reduce costs and material waste, as well as to aid in rapid prototyping and testing. Except for the diaphragm, the entire body and inner parts are printed with ABS material. The entire body is sealed with hot glue using a glue gun, making the FBG sensor part completely waterproof. Also, there is no physical contact with a measured liquid medium.

REFERENCES

[1] R. Kashyap, *Fiber Bragg Gratings*. Cambridge, MA, USA: Academic Press, 2009.

[2] A. Othonos, "Fiber Bragg gratings," *Rev. Sci. Instruments*, vol. 68, no. 12, pp. 4309–4341, 1997.

[3] K. O. Hill and G. Meltz, "Fiber Bragg grating technology fundamentals and overview," *J. Lightw. Technol.*, vol. 15, no. 8, pp. 1263–1276, 1997.

[4] P. S. Reddy et al., "Teflon-coated fiber Bragg grating sensor for wide range of temperature measurements," *J. Optoelectron. Adv. Mater.*, vol. 12, pp. 2040–2043, 2010.

[5] W. Zhang, X. Dong, Q. Zhao, G. Kai, and S. Yuan, "FBG-type sensor for simultaneous measurement of force (or displacement) and temperature based on bilateral cantilever beam," *IEEE Photon. Technol. Lett.*, vol. 13, no. 12, pp. 1340–1342, Dec. 2001.

[6] P. S. Reddy et al., "Method for enhancing and controlling temperature sensitivity of fiber Bragg grating sensor based on two bimetallic strips," *IEEE Photon. J.*, vol. 4, no. 3, pp. 1035–1041, Jun. 2012.

[7] V. S. C. S. Vaddadi, S. R. Parne, V. Vijeesh, S. Gandi, and L. R. Cenkeramaddi, "Design and implementation of density sensor for liquids using fiber Bragg grating sensor," *IEEE Photon. J.*, vol. 14, no. 1, Feb. 2022, Art. no. 6804106.

[8] Z. Zhou and J. Ou, "Development of FBG sensors for structural health monitoring in civil infrastructures," in *Proc. Sens. Issues Civil Struct. Health Monit.*, 2005, pp. 197–207.

[9] T. S. Mansour and F. M. Abdulhussein, "Dual measurements of pressure and temperature with fiber Bragg grating sensor," *Al-Khwarizmi Eng. J.*, vol. 11, no. 2, pp. 86–91, 2015.

[10] J. Huang, Z. Zhou, D. Zhang, and Q. Wei, "A fiber Bragg grating pressure sensor and its application to pipeline leakage detection," *Adv. Mech. Eng.*, vol. 5, 2013, Art. no. 590451.

[11] V. Mishra, N. Singh, U. Tiwari, and P. Kapur, "Fiber grating sensors in medicine: Current and emerging applications," *Sensors Actuators A: Phys.*, vol. 167, no. 2, pp. 279–290, 2011.

[12] L. Schenato et al., "Highly sensitive FBG pressure sensor based on a 3D-printed transducer," *J. Lightw. Technol.*, vol. 37, no. 18, pp. 4784–4790, 2019.

[13] M.-F. Liang, X.-Q. Fang, G. Wu, G.-Z. Xue, and H.-W. Li, "A fiber Bragg grating pressure sensor with temperature compensation based on diaphragm-cantilever structure," *Optik*, vol. 145, pp. 503–512, 2017.

[14] W. Zhang, F. Li, and Y. Liu, "FBG pressure sensor based on the double shell cylinder with temperature compensation," *Measurement*, vol. 42, no. 3, pp. 408–411, 2009.

[15] V. S. C. S. Vaddadi, S. R. Parne, S. Afzulpurkar, S. P. Desai, and V. V. Parambil, "Design and development of pressure sensor based on fiber Bragg grating (FBG) for ocean applications," *Eur. Phys. J. Appl. Phys.*, vol. 90, no. 3, 2020, Art. no. 30501.

[16] O. F. Ameen, M. H. Younus, M. Aziz, A. I. Azmi, R. R. Ibrahim, and S. Ghoshal, "Graphene diaphragm integrated FBG sensors for simultaneous measurement of water level and temperature," *Sensors Actuators A: Phys.*, vol. 252, pp. 225–232, 2016.

[17] Z. Hong-Kun, Z. Yong, Z. Qiang, and L. Ri-Qing, "High sensitivity optical fiber pressure sensor based on thin-walled oval cylinder," *Sensors Actuators A: Phys.*, vol. 310, 2020, Art. no. 112042.

[18] Y. Liu, Z. Guo, Y. Zhang, K. S. Chiang, and X. Dong, "Simultaneous pressure and temperature measurement with polymer-coated fibre Bragg grating," *Electron. Lett.*, vol. 36, no. 6, pp. 564–566, 2000.

[19] Q. Zhao et al., "Adhesive-free bonding fiber optic Fabry–Perot pressure sensor based on oxy-hydrogen flame welding and spiral tube," *Opt. Commun.*, vol. 476, 2020, Art. no. 126307.

[20] Y. Ouyang, J. Liu, X. Xu, Y. Zhao, and A. Zhou, "Phase-shifted eccentric core fiber Bragg grating fabricated by electric arc discharge for directional bending measurement," *Sensors*, vol. 18, no. 4, 2018, Art. no. 1168.

[21] Y. Cui, Y. Jiang, T. Liu, J. Hu, and L. Jiang, "A dual-cavity Fabry–Pérot interferometric fiber-optic sensor for the simultaneous measurement of high-temperature and high-gas-pressure," *IEEE Access*, vol. 8, pp. 80582–80587, 2020.

[22] L. Schenato, J. P. Aguilar-Lopez, A. Galtarossa, A. Pasuto, T. Bogaard, and L. Palmieri, "A rugged FBG-based pressure sensor for water level monitoring in dikes," *IEEE Sensors J.*, vol. 21, no. 12, pp. 13263–13271, Jun. 2021.

[23] Q. Fan et al., "Design and investigation of the fiber Bragg grating pressure sensor based on square diaphragm and truss-beam structure," *Opt. Eng.*, vol. 58, no. 9, 2019, Art. no. 097109.

[24] P. V. Rao, K. Srimannarayana, P. Kishore, M. S. Shankar, D. Sengupta, and P. S. Reddy, "Development of high sensitivity pressure sensor using reduced clad FBG," in *Proc. Opt. Sens. Detection II*, 2012, Art. no. 84392G.

[25] C. Hong, Y. Zhang, and L. Borana, "Design, fabrication and testing of a 3D printed FBG pressure sensor," *IEEE Access*, vol. 7, pp. 38577–38583, 2019.

[26] C. A. Díaz et al., "Liquid level measurement based on FBG-embedded diaphragms with temperature compensation," *IEEE Sensors J.*, vol. 18, no. 1, pp. 193–200, Jan. 2018.

[27] S. Timoshenko and S. Woinowsky-Krieger, *Theory of Plates and Shells.* New York, NY, USA: McGraw-Hill, 1959.

[28] J. Huang, Z. Zhou, X. Wen, and D. Zhang, "A diaphragm-type fiber Bragg grating pressure sensor with temperature compensation," *Measurement*, vol. 46, no. 3, pp. 1041–1046, 2013.

[29] Y. Xiong, J. He, W. Yang, L. Sheng, W. Gao, and Y. Chen, "Research on FBG pressure sensor of flat diaphragm structure," in *Proc. Int. Conf. Meas., Inf. Control*, 2012, pp. 787–790.

[30] T. Guo, X. Qiao, Z. Jia, Q. Zhao, and X. Dong, "Simultaneous measurement of temperature and pressure by a single fiber Bragg grating with a broadened reflection spectrum," *Appl. Opt.*, vol. 45, no. 13, pp. 2935–2939, 2006.

[31] C. Marques, A. Pospori, D. Sáez-Rodríguez, K. Nielsen, O. Bang, and D. Webb, "Aviation fuel gauging sensor utilizing multiple diaphragm sensors incorporating polymer optical fiber Bragg gratings," *IEEE Sensors J.*, vol. 16, no. 15, pp. 6122–6129, Aug. 2016.

[32] J. Huang, Z. Zhou, Y. Tan, M. Liu, and D. Zhang, "Design and experimental study of a fiber Bragg grating pressure sensor," in *Proc. Int. Conf. Innov. Des. Manuf.*, 2014, pp. 217–221.

[33] M. Fajkus et al., "Pressure membrane FBG sensor realized by 3D technology," *Sensors*, vol. 21, no. 15, 2021, Art. no. 5158.

[34] G. Allwood, G. Wild, A. Lubansky, and S. Hinckley, "A highly sensitive fiber Bragg grating diaphragm pressure transducer," *Opt. Fiber Technol.*, vol. 25, pp. 25–32, 2015.

[35] E. Vorathin, Z. Hafizi, A. Aizzuddin, and K. S. Lim, "A natural rubber diaphragm based transducer for simultaneous pressure and temperature measurement by using a single FBG," *Opt. Fiber Technol.*, vol. 45, pp. 8–13, 2018.